

Sucrose Clusters Exhibiting a Magic Number in Dilute Aqueous Solutions

Stanley L. Kaufman* and Frank D. Dorman†

TSI Incorporated, 500 Cardigan Road, St. Paul, Minnesota 55126

Received January 18, 2008. Revised Manuscript Received June 20, 2008

We report clustering of sucrose molecules in dilute aqueous solutions, based on measurements of the electrical mobility spectrum of singly charged airborne clusters produced by electrospraying the solution. The spectrum contains peaks with a smooth envelope, except for one peak which has about twice the amplitude of the envelope. The mobility at this peak is found to be somewhat higher than would be expected based on the rest of the sequence, suggesting a more compact structure for this cluster. This "magic" peak is prominent for basic, but not acidic, solutions. It is argued that these observations demonstrate the existence of clusters of many sizes in the solution prior to electrospraying, including the "magic" cluster. A simplified model is presented which reproduces the observed features.

Dilute solutions of single, nondissociating compounds are usually assumed to be random spatial distributions of individual solute molecules in the solvent. In this work we report experimental evidence of clustering of sucrose molecules even at 20 $\mu\text{mol/L}$, with a favored "magic" cluster number. We measured the electrical mobility spectrum of an aerosol of sucrose clusters formed by spraying and drying a dilute sucrose solution, using a differential mobility analyzer (DMA).^{1–5} Within the expected Poisson envelope of peaks due to clusters of successively increasing numbers of sucrose molecules, the spectrum includes a prominent peak whose existence furthermore depends on the solution pH. From these observations and consideration of details of the electrospray process, we argue that clusters of sucrose molecules of all sizes must exist in the solution before spraying.

Mathlouthi⁶ studied correlations of sucrose molecules in solution by X-ray diffraction. McCain and Markley⁷ studied sucrose in solution by NMR. Both of these studies were carried out at concentrations approaching saturation, where effects of

neighboring sucrose molecules would be expected to be important. Immel and Lichtenthaler⁸ developed a molecular-dynamics model of sucrose in a water environment. None of these authors appear to have considered the possible formation of sucrose molecular clusters. Penn and Banfield⁹ and Banfield et al.¹⁰ observed crystallization by "oriented attachment" in which nanocrystals combine to form larger single crystals.¹¹ The clusters observed in the present work may be regarded as nanocrystals of sucrose, which one may speculate could take part in a similar process.

We applied the charge-reduced monodisperse electrospray method^{12–16} to dilute solutions of sucrose in 20 mM ammonium acetate, for which the expected number of sucrose monomers per spray droplet was in the range 10–100¹⁷ (Ammonium acetate is volatile and is added to provide conductivity to control the electrospray operation). A 5-mCi ²¹⁰Po alpha source in the electrospray neutralizing chamber provided air ions to reduce the charge of the electrospray droplets during droplet evaporation. The resulting sucrose clusters have approximately the Fuchs charge distribution^{18,19} according to which nearly all charged particles in this size range carry a single charge. Under these

* To whom correspondence should be addressed. E-mail: skaufman@tsi.com.

† Retired. Present address: 301 Burntside Drive, Minneapolis, MN 55422.

(1) The flow-through aerosol differential mobility analyzer(DMA)^{2,3} determines the mobility of transmitted particles by their migration across a laminar flow under the influence of an electric field controlled by an applied potential. The DMA used here was designed by Eichler.^{4,5} The parameters which determine the transmitted mobility are the sheath flow (292 L/min), the applied potential, and the geometric dimensions of the DMA. The DMA outlet contains a precipitator whose collector is connected to an electrometer to measure the current of charged particles transmitted through the outlet slit. The applied potential was controlled by an MS-DOS program which recorded the potential and the electrometer current in a file for subsequent processing. The potential values were calibrated using a traceable high-voltage divider and a digital voltmeter, and the calibration was used to correct the recorded values. To calculate the mobility at each potential, we used the formula of Knutson and Whitby.² The pressure in the analyzer was 0.95 atm at the flow rates used, and the mobility was assumed to be inversely proportional to pressure to obtain the mobility values at standard conditions.

(2) Knutson, E. O.; Whitby, K. T. *J. Aerosol Sci.* **1975**, *6*, 443–451.

(3) Knutson, E. O.; Whitby, K. T. *J. Aerosol Sci.* **1975**, *6*, 453–460.

(4) T. Eichler, Senior Graduation Thesis, Fachhochschule Offenburg (1997); J. Fernandez de la Mora, L. de Juan, and T. Eichler, J. Rosell, U.S. Patent 5,869,831 (1999).

(5) Fernandez de la Mora, J.; de Juan, L.; Eichler, T.; Rosell, J. *Trends Anal. Chem.* **1998**, *17*, 328–339.

(6) Mathlouthi, M. *Carbohydr. Res.* **1981**, *91*, 113–123.

(7) McCain, D. C.; Markley, J. L. *Carbohydr. Res.* **1986**, *152*, 73–80.

(8) Immel, S.; Lichtenthaler, F. W. *Liebigs Ann.* **1995**, 1925.

(9) Penn, R. L.; Banfield, J. F. *Geochim. Cosmochim. Acta* **1999**, *63*, 1549.

(10) Banfield, J. F.; Welch, S. A.; Zhang, H.; Ebert, T. T.; Penn, R. L. *Science* **2000**, *289*, 751.

(11) Alivisatos, A. P. *Science* **2000**, *289*, 736.

(12) S. L. Kaufman, F. Zarrin, F. Dorman, U. S. Patent No. 5,247,842 (1993).

(13) Lewis, et al. *Anal. Chem.* **1994**, *66*, 285.

(14) Chen, D.-R.; Pui, D. Y. H.; Kaufman, S. L. *J. Aerosol Sci.* **1995**, *26*, 963–977.

(15) Kaufman, S. L.; Skogen, J. W.; Dorman, F. D.; Zarrin, F.; Lewis, K. C. *Anal. Chem.* **1996**, *68*, 1895–1904 (see Correction: *Anal. Chem.* **68**, 3073 (1996)).

(16) Scaif, M.; Westphall, M. S.; Krause, J.; Kaufman, S. L.; Smith, L. M. *Science* **1999**, *283*, 194–197.

(17) The capillary liquid flow was 65 nL/min, and the spray was stable at typically 2.8 kV and 230 nA. The air flow through the electrospray chamber was 6 L/min, with a 0.15 L/min flow of CO₂ surrounding the needle to prevent corona discharge. We determined the primary spray droplet diameter to be 160 nm, using the method described by Lewis et al.¹³ and by Chen et al.¹⁴ A solution of 1.6 mg/mL of reagent-grade sucrose in 20 mM ammonium acetate was diluted as required into 20 mM ammonium acetate, with pH adjusted as desired by adding either concentrated ammonia or glacial acetic acid. The liquid conductivity was 0.2 S/m for all pH values used. All solutions were kept refrigerated before use.

(18) Fuchs, N. A. *Geophys. Pura Appl.* **1963**, *56*, 185.

(19) Wiedensohler, A. *J. Aerosol Sci.* **1988**, *19*, 387.

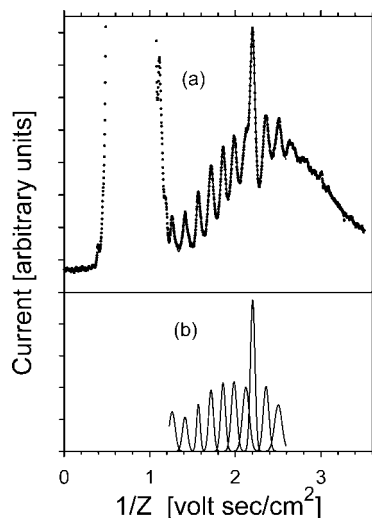


Figure 1. (a) Electrometer current versus inverse mobility in air, for 6.4 $\mu\text{g/mL}$ of sucrose in 20 mM ammonium acetate at pH 8.6. Plotted in this way, the larger clusters appear toward the right. Points: raw data; curve: sum of Gaussian peaks fitted in region shown. The offscale composite peak to the left of the series of sucrose cluster peaks is due to small "air ions" resulting from alpha bombardment of gas in the electrospray neutralizing chamber. (b) Individual Gaussian peaks which are summed in the fitted function. A linear background, not shown, was included in the fit.

conditions the mobility spectrum directly reflects the size spectrum of the aerosol.

Figure 1a shows the electrical mobility spectrum of a sample at basic pH. The composite peak at the left, present only when the alpha source is in place, is attributed to air ions. To the right of the air-ion group is a series of regularly spaced peaks, which are present only when the electrosprayed solution contains sucrose (and with the alpha source present). These peaks are attributed to sucrose clusters, each successive peak representing clusters of one additional sucrose molecule. The larger peak near the center of the group is the magic number sucrose cluster. Figure 2 shows that when the sucrose concentration was increased, the envelope of sucrose cluster peaks shifted toward larger sizes, but the magic-cluster peak remained in the same position. For increasing cluster size, the relative separation of adjacent peaks decreases, so that for the larger clusters the DMA is no longer able to resolve adjacent peaks. However, Figure 2 shows that the magic-cluster peak remains visible on the rising slope of the structure even when the peak of the envelope has been shifted well into the unresolved range. Figure 3 shows the influence of solution pH. The magic-cluster peak is present for basic pH, but is absent for acidic pH.

The data points of Figure 1a were fitted in the sucrose cluster region using a sum of ten Gaussian functions (Figure 1b) to determine the best-fit mobility in air for each peak. The mobilities of all of the clusters in the fitted region of Figure 1, corrected to standard pressure, are listed in Table 1. The mobility at the magic peak is found to be somewhat higher than would be expected based on the rest of the sequence, suggesting a more compact structure for this cluster.

It would be interesting to know the value of M , the number of sucrose molecules in the magic peak. Vitamin B-12 clusters observed in the same apparatus,²⁰ which did not exhibit a magic-cluster peak, included the monomer, so the number of molecules in each cluster could be found simply by counting the peaks. This was not possible for sucrose since the monomer and low-

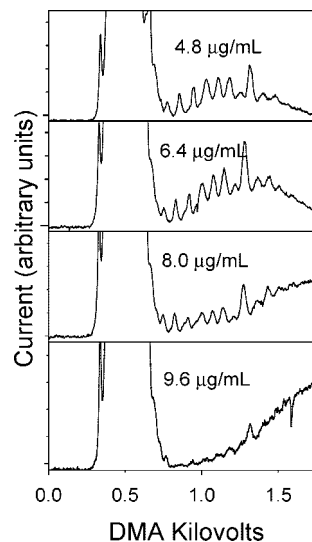


Figure 2. Sucrose spectra for varying sucrose concentrations in pH 8.4 20 mM ammonium acetate. The abscissa is the potential applied to the DMA, which is proportional to inverse mobility. The flow rate in the DMA was subject to some drift during these runs, resulting in small run-to-run variations in the peak positions. The downward spike in the lower plot was an electrical transient.

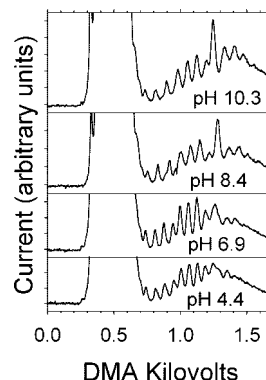


Figure 3. Sucrose peaks for varying buffer pH, at 6.4 $\mu\text{g/mL}$. The 20 mM ammonium acetate buffer pH was adjusted by adding either ammonia or glacial acetic acid. The "magic" peak is prominent only for basic pH values.

Table 1. Mobilities of the Observed Clusters in Air^a

number	mobility [$\text{cm}^2/\text{V} \cdot \text{s}$]
5	0.792
6	0.708
7	0.637
8	0.582
9	0.538
10	0.504
11	0.471
12*	0.454
13	0.424
14	0.400

^a The mobilities obtained by fitting a sum of Gaussian peaks to the data in Figure 1. A linear background was assumed in the fit. The values have been corrected to atmospheric pressure.¹ The asterisk denotes the "magic number" cluster, assumed here to be 12. See text for discussion of the problem of assigning the absolute sucrose number.

order clusters of this smaller molecule are obscured by the air-ion group. We attempted to determine M by additional analysis and comparison with other data. Following F. de la Mora et al.,²¹ we fitted the data to a model appropriate to the slip regime (cluster dimensions \ll gas mean free path), in which mobility of spheres

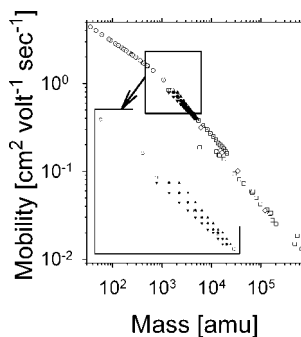


Figure 4. Comparison of sucrose cluster mobilities with other available mobility data. Open circles (dotted circles): Kilpatrick's negative (positive) air-ion data²² as interpreted by Tammet.²³ Open squares: protein data of Kaufman et al.;¹⁵ Open diamonds: DNA oligomer data of Mouradian et al.²⁴ Dotted squares: vitamin B-12 clusters.²⁰ Sucrose cluster data (this work) is shown as filled circles (assuming $M = 12$) and as triangles (assuming $M = 11$ and $M = 13$). See text for discussion.

(representing the clusters) is inversely proportional to the square of the sum of the sphere radius and the effective radius of the gas molecules. The linear dependence fitted was $Z_j^{-1/2} = A + B(N_j(M))^{1/3}$, where Z_j is the observed electrical mobility of the j th cluster (counted from the first observed peak) and $N_j(M)$ is the number of sucrose molecules in the j th cluster for an assumed value of the magic number M . The value of A is related to the gas molecule collision radius, and B is related to the effective radius of the sucrose monomer. Such fits were made for assumed values of M from 9 to 15. The best straight-line fit, as judged by either correlation coefficient or F-statistic, was obtained for $M = 12$, but a straight line could not be ruled out on this basis alone for the range $11 \leq M \leq 13$. For $M = 13$, the intercept A is negative, a nonphysical situation which would appear to rule out this value. For $M = 12$ the intercept is $0.0132 \pm 0.0146 \text{ V}^{1/2} \cdot \text{s}^{1/2} \cdot \text{cm}^{-2}$, consistent with zero. For $M = 11$ the intercept is $0.159 \pm 0.015 \text{ V}^{1/2} \cdot \text{s}^{1/2} \cdot \text{cm}^{-2}$. Tammet's theory²³ as applied by F. de la Mora et al.,²¹ yields an effective molecular diameter of $0.225 \pm 0.021 \text{ nm}$ for $M = 11$, smaller than the 0.53 nm given by F. de la Mora et al.²¹ For $M = 12$ the effective gas molecular diameter is consistent with zero. The present sucrose data are for masses that lie between the those analyzed by F. de la Mora et al.,²¹ where polarization and recoil are negligible, and the air-ion data of Kilpatrick²² analyzed by Tammet²³ where these effects are significant. Our clusters are thus in a range where the linear dependence in the fits just described could break down. We therefore studied, without any assumed functional dependence, the systematics of mobility versus mass over the range including all of the Kilpatrick²² data as restored by Tammet,²³ the sucrose clusters of this work, the protein data of Kaufman et al.,¹⁵ the vitamin B-12 data,²⁰ and the DNA oligomer data of Mouradian et al.²⁴ As in the previous analysis, the mass of the j th cluster was assumed to be an integer multiple ($N_j(M)$) of the sucrose mass 342.3 Da , with the magic peak assumed to be $M = 11, 12$, or 13 . The result is plotted in Figure 4. The sucrose cluster points assuming $M = 12$ connect most smoothly with the larger ions in the Tammet/Kilpatrick data. The data on proteins and DNA establish an overall slope, but do not significantly constrain M , due to the appreciable scatter of the protein data as well as apparent systematic differences between proteins, DNA oligomers, and

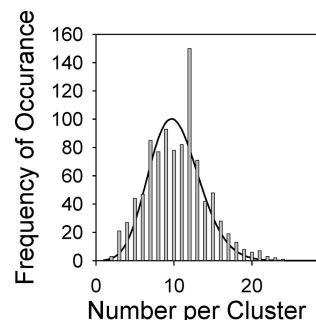


Figure 5. Vertical bars: result of a Monte Carlo simulation of the process of cluster formation in solution, starting with 10^4 monomers and using 5.12×10^8 iterations. The probability of aggregation $j + \text{monomer} \Rightarrow j + 1$ for each j -cluster ($j = 1.50$), for each iteration, was 0.5 ; the probability of dissociation $j \Rightarrow j - 1 + \text{monomer}$ for each j -cluster was $1.5625 \times 10^{-5} j^{2/3}$, i.e., proportional to cluster surface area or the number of surface monomers. For $j = 12$ only, both coefficients were reduced by a factor of 2. Solid curve: reference Poisson distribution with mean 10.2 and total number of clusters 800 . The simulation reproduces the main features in the observed mobility spectra, and thus supports the idea that relatively simple solution processes can result in the observed cluster distribution.

larger Vitamin B-12 clusters. The vitamin B-12 dimer and trimer coincide very closely in mass with two of the sucrose peaks under the $M = 12$ assumption, and their mobilities are also nearly coincident. The vitamin B-12 monomer falls closer to the $M = 11$ series, but it also appears to be systematically slightly out of line with the remaining vitamin B-12 cluster mobilities.

Thus, analysis based on the linear fits and the comparison with the air-ion, protein, and vitamin B-12 cluster data cannot provide a satisfactory determination of the exact number of sucrose molecules in the magic cluster of Figure 1. The best that can be said is that it must be either 11 or 12.

The clusters must originate either in solution, in the electrospray process, or in the gas phase. The transit time of liquid through the jet in the cone-jet electrospray is estimated from the electrospray parameters and plume geometry to be less than $0.46 \text{ microseconds}$. If the molecules are not clustered before entering the jet, the rate of diffusive encounters between sucrose molecules at $6.4 \mu\text{g/mL}$ ($83 \mu\text{M/L}$) in solution is $4 \cdot 10^6 \text{ s}^{-1}$, giving a mean of less than 2 encounters during the transit time through the electrospray jet, hardly sufficient for aggregates of the observed sizes to form during transit. After the spray droplets have left the tip, they separate rapidly due to their high initial charge and begin to evaporate. Their subsequent interaction is governed by diffusive coagulation. Droplets are produced at a rate of about $10^9/\text{s}$, which at the 6 L/min air flow rate results in droplet or residue particle concentration of $10^{13}/\text{m}^3$. Assuming complete evaporation and a final cluster or residue diameter of 1 nm and using Smolochowski's coagulation coefficient, the mean time between diffusive encounters would thus be $> 1.5 \text{ s}$, longer than the time the aerosol spends in the apparatus. Thus it is highly unlikely that interactions in the aerosol state can affect the cluster size distribution. We conclude that the magic-number clusters must be formed in solution rather than in the spray process or in the aerosol phase after spraying.

If individual sucrose molecules were isolated and randomly distributed in solution, and if the electrosprayed droplets were equal-volume random samples of the liquid, then the number of sucrose molecules contained in each droplet would follow a Poisson distribution whose parameter is the mean number of sucrose molecules per droplet. Although the droplets are not perfectly monodisperse, they have a narrow size distribu-

(21) de la Mora, F.; de Juan, L.; Liedtke, K.; Schmidt-Ott, A. *J. Aerosol Sci.* **2003**, *34*, 79–98.

(22) Kilpatrick, W. D.; W. D. *Proc. 19th Annual Conf. Mass Spectrosc.* **1971**, 320–325.

(23) Tammet, H. *J. Aerosol Sci.* **1995**, *26*(3), 459–475.

(24) Mouradian, S.; et al. *Anal. Chem.* **1997**, *69*, 919–925.

tion, so the observed mobility distribution should have a smooth envelope closely resembling the Poisson distribution. Indeed, the vitamin B-12 results²⁰ show just such a distribution, with the exception of the B-12 monomer which may be produced by ion evaporation. The one-component Poisson model cannot account for the existence of a prominent magic-number peak, nor does it correctly predict the location of the envelope maximum. For 6.4 $\mu\text{g/mL}$ of sucrose, the predicted mean number of sucrose molecules per 160-nm diameter droplet is 24, whereas the observed envelope maximum (ignoring the magic peak) occurs at about 12 molecules. This observation itself already suggests a nonrandom distribution of monomers in the solution.

Simple models were used to identify the coarse mechanisms that might be responsible for the magic number clusters in solution. For modeling purposes, $M = 12$ was assumed. A two-component model in which the solution contains monomers and clusters of 12 sucrose molecules, or monomers and a larger impurity molecule, randomly distributed in the solution, also fails to predict the observed pattern. In this model the joint probability for a droplet to contain m 12-clusters and n monomers is the product of the two Poisson probabilities with parameters corresponding to the two concentrations. When expressed as the probability for a droplet to contain $j = 12m + n$ monomers, the resulting distribution is a series of cluster peaks with an envelope of broad "humps" each containing many peaks, and each corresponding to one additional 12-mer, not at all resembling the observed distribution.

Finally, suppose that clusters of all sizes exist in equilibrium in solution prior to spraying, with a mean number per cluster

proportional to the total concentration of monomers (aggregated or not) present. For the conditions of the experiment, a droplet would then contain on average one or fewer single clusters (of any size). If a cluster of 12 is more stable than its neighbors, the population of 12-clusters will be larger, and the observed spectrum can be reproduced. This was verified by means of a Monte Carlo simulation, shown in Figure 5. This model also resolves the question of the location of the maximum for the smooth part of the distribution envelope in Figure 1 at 12 versus 24, since the mean number of monomers is now determined in part by the relative population of magic clusters.

A brief search was made, at pH 8.6 only, for magic clusters in two other disaccharides. Both maltose and lactose showed multiple-peak cluster structure, but the distributions were Poisson-like and showed no evidence of a magic-number cluster. More systematic investigation of these and other disaccharides is called for.

Bound solvent molecules, including ions from the ammonium acetate, might play a role in cluster formation. The DMA does not have sufficient resolution to study adducts, but this information should be accessible by mass spectrometry of the clusters, using charge reduction as in Scalf et al.¹⁶

Acknowledgment. The authors thank Professor Juan Fernandez de la Mora of Yale University for the loan of the high-resolution DMA used in this work and Klaus Liedtke of Yale and Duisburg Universities for assistance in setting it up.

LA800177M